

# Permeability of Basalt Through the Brittle-Ductile Transition, Implications for Superhot Rock Geothermal

Gabriel G. Meyer<sup>1</sup>, Geoffrey Garrison<sup>2</sup> and Marie Violay<sup>1</sup>

<sup>1</sup>Laboratory of experimental Rock Mechanics, Ecole Polytechnique Fédérale de Lausanne, Lausanne, Switzerland

<sup>2</sup>AltaRock Energy, Inc. Seattle, USA

[gabriel.meyer@epfl.ch](mailto:gabriel.meyer@epfl.ch)

**Keywords:** Brittle, ductile, deformation, permeability, geothermal energy, superhot rock

## ABSTRACT

Superhot Rock (SHR) geothermal projects (e.g., Japan Beyond-Brittle Project, Iceland Deep Drilling Project, and Newberry Volcano) seek to extract heat from geothermal reservoirs where water reaches a supercritical state ( $\geq 400$  °C). Exploiting such a resource could multiply the electrical power delivered by geothermal wells by almost an order of magnitude. However, SHR reservoirs are in semi-brittle to ductile rocks where fluid flow, porosity, permeability, and rock mechanics are still poorly understood. The Newberry SHR project has engaged EPFL Lausanne (CH) to conduct experiments at their brand-new, internally heated, gas-confining triaxial apparatus to deform reservoir-type samples under realistic SHR temperature, pressure, and strain rate conditions. Deep well core samples (40  $\times$  20 mm) of basalts (porosities of 1–15%) from Newberry Volcano were subjected to increasing confinement pressure (25–100 MPa) and temperature (20–500 °C) while continuously recording gas permeability via harmonic permeability. Additionally, triaxial deformation experiments were done at strain rates of  $10^{-6}$ , confinement up to 100 MPa, temperature up to 500 °C, and up to 8% strain while recording permeability. Samples were ductile (e.g., no localization of strain) at relatively low pressure–low temperature conditions (100 MPa, 200 °C). Moreover, permeability in samples subjected to hydrostatic conditions rapidly decreased several orders of magnitude from an initial value of  $5.10^{-20}$  m<sup>2</sup> to less than  $10^{-22}$  m<sup>2</sup> at 50 MPa and 200 °C, effectively impermeable. Thus, permeability decreases rapidly in the ductile regime with strain to reach below measurable values at around 3% strain, and it remains so during subsequent semi-brittle flow up to 8% strain. We interpret this rapid decay of permeability as a result of the conjoined effect of ductile pore collapse and plastic deformation of the poorly crystalline matrix present in the sample. Our results constitute a new advancement in geoengineering as permeability during ductile deformation had never been continuously recorded during ductile deformation before. These insights further underline the need for advanced, sustainable reservoir engineering techniques in order to extract heat from high enthalpy geothermal reservoirs.

## 1. INTRODUCTION

With the advent of the climate crisis, finding new sources of renewable energy is critical and the focus of intense research and engineering developments. Geothermal is one such sources: it is renewable, sustainable and nearly ubiquitous (albeit variable depending on the geological context) on Earth. The most limiting factor to a geothermal plant performance is temperature which is typically around 250 to 300 °C. Recently, with the discovery by the Iceland Deep Drilling project of a supercritical geothermal reservoir (450C) directly above a magma body at Krafla (Elders et al., 2014) a new avenue for geothermal has been opened: that of super-hot reservoirs (SHR). Exploiting such reservoirs could multiply the power output of plants by a factor 10 (Friðleifsson et al., 2014). Following in this wake, the Japan Beyond-Brittle Project (JBBP), the Taupo Volcanic Zone-Deep geothermal drilling project in New Zealand (TVZ-DGDP) (Bignall & Carey, 2011) and NDDP project at the Newbury volcano (Cladouhos et al., 2018), proposed a similar concept in engineering development where geothermal reservoirs are created in semi-brittle/ductile rocks. Creating geothermal systems in ductile rocks has the advantage of having simpler designs and control owing to homogeneous reservoir properties and stress states. Moreover, ductile rocks being generally aseismic, exploiting these reservoirs could be a way to circumvent induced seismicity.

However, the hydraulic properties of ductile rocks, particularly porosity and permeability are still mostly unknown. Permeability is the main controlling parameter to the heat transfer between magma bodies and hydrothermal systems (Driesner & Geiger, 2007; Fournier, 1999; Hayba & Ingebritsen, 1997; Prejean & Haney, 2014; Weis, 2015). Recent numerical simulations have shown that the BDT (brittle to ductile transition) and the temperature dependence of permeability play the key role on the maximum temperature and size of geothermal reservoirs (Jolie et al., 2021; Scott et al., 2015). It is usually believed to vanish with increasing temperature and pressure, when rocks switch from deforming via microcracking and fractures to deforming by homogenous flow, but this has never been observed in the laboratory and no constraint currently exist on the relationship between temperature dependent rock deformation and permeability decay, and their dependence in rate and time. Understanding constraints is a first step towards being able to engineer SHR geothermal reservoirs

Here we present extremely early data obtained with a newly designed, internally heated gas triaxial apparatus with fluid flow capabilities. We conducted experiments on deep core samples of Newberry Volcano basalts (NBB) under conditions spanning the brittle-ductile transition. We conducted both dry experiments to constraint the rheological envelope of the samples and experiments with pore fluid to record permeability. We show that strain rate is a critical control on the brittle ductile transition of NBB and that, in the ductile regime, permeability rapidly decreases during deformation until the samples are effectively impermeable. These data being very immature are still prone to changes and the dataset will be expanded upon in the future.

## 2. SAMPLES AND METHOD

### 2.1 Newberry volcano basalts

In the present work, we focus on rock samples from the Newberry SHR project in Oregon. We acquired deep cores from well GEO-N2 at depth ranging from 1110 to 1350 m (3583 – 4343 feet; Figure 1) hereafter denominated by their depth in feet. Drill hole GEO-N2 was spudded August 15, 1986, at an elevation of 1,779 m on the west flank of Newberry volcano about 2.8 km outside the western rim of the caldera and just east of the Newberry EGS Demonstration Project well NWG55-29. From the cores, we extracted cylindrical samples of 20 mm in diameter which we then cut to 41 mm in length. Next, we rectified the samples with a surface grinder to ensure parallelism of the loading faces. Not all core sections were of the same length and some were more fractured than others (likely due to decompression), for these reasons, the number of exploitable samples extracted from each section varies from 3 to 5.

Samples are visually similar, light gray to light brown in color and seem relatively fine grained and homogeneous. Some sections show evident signs of alteration with veins and vesicles filled with milky white minerals. Section 3583 is very altered and the surface of the samples being crisscrossed by a dense array of whitish veins (Figure 1).

Prior to testing, we conducted a thorough bench-top investigation of the physical properties of every sample by weighting them dry, measuring the elastic wave speed velocities and using a gas pycnometer to measure porosity. Data are gathered in Figure 1. Overall, the basalt samples seem to fall into two categories. Those obtained at depth above 3900 feet show high porosities ranging from 10 to 15% with P wave speeds of 3500 m/s on average and S wave speeds of 2300 m/s on average. Those from below 3900 feet depth show significantly lower porosities, being 8% on average at 4010 feet and reaching close to 0% at 4343 feet. Conversely, in these samples, P wave speeds increase from 3500 m/s on average up to 4500 m/s and S wave speeds from 2400 m/s on average to 3100 m/s from 4010 to 4343 feet (Figure1).

In order to accurately determine the composition of the different cores and to assess the degree and impact of alteration, we conducted X-ray diffractometry on powders from two select cores (Figure 2). We chose cuttings from a visually fresh and a visually altered layer of the basalt (i.e., 3124 and 3583 feet respectively). Results show that the two basalts are somewhat different: the fresh basalt is 48% Na plagioclase, 17% phyllosilicates, 7.5% quartz and 27% of the mass couldn't be identified (most likely glassy material). On the other hand, the altered core is 67% Na Plagioclase, 8% phyllosilicates and 6 % quartz while 18.5% of the mass couldn't be determined. Therefore, despite originating from the same well and from relatively close depths, some substantial compositional differences exist between our cores. For this reason, we focused our investigation on sample batches extracted from single cores.

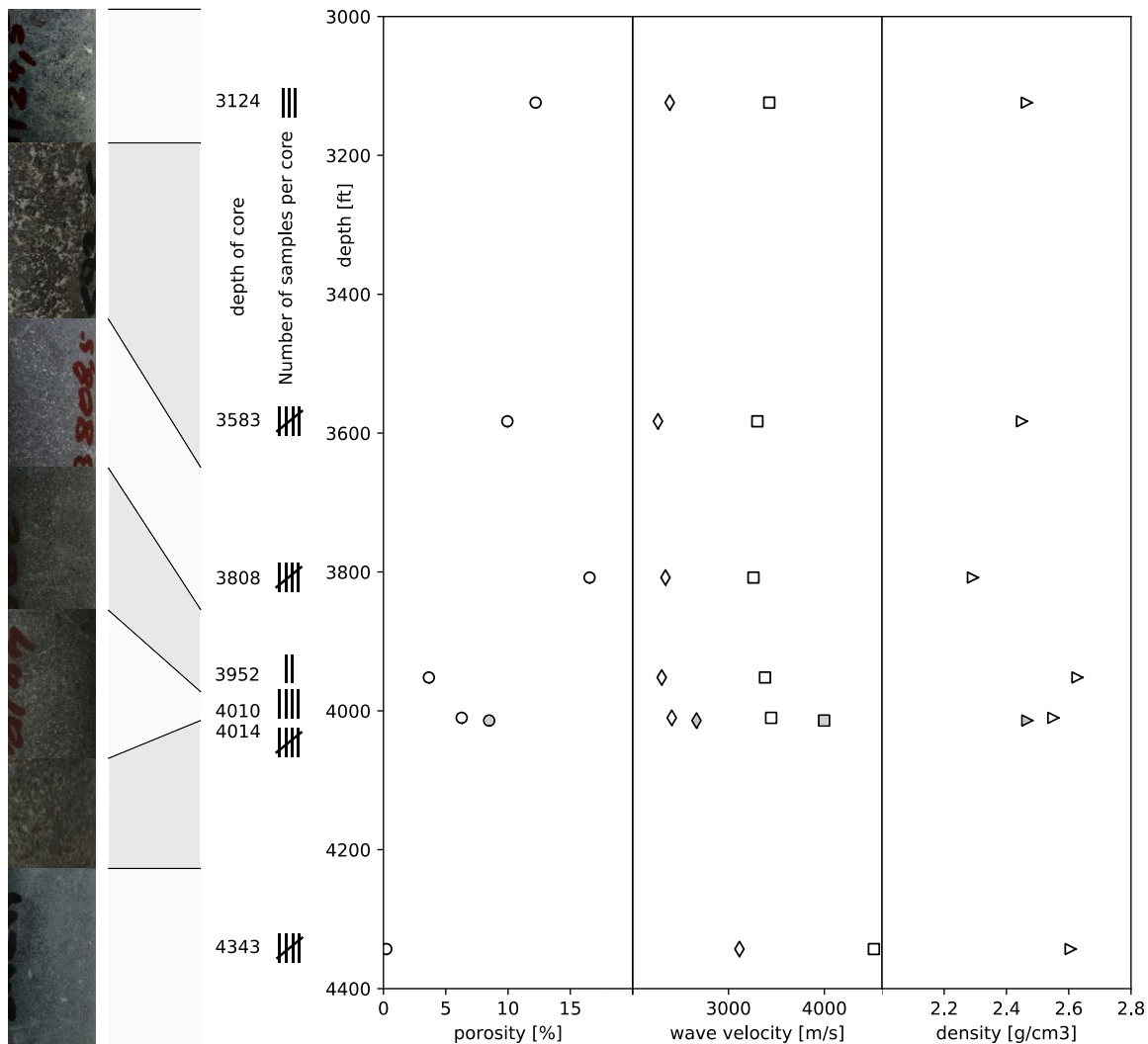


**Figure 1: A collection of physical properties of the GEO-N2 well basalt cores. Leftmost is a collage of representative extracted samples for rapid visual comparison. Porosity was measured using helium pycnometry. Wave speeds were recorded on the benchtop using piezoelectric sensors (Olympus 1MHz). Density was calculated using the dry mass of the sample and the skeleton volume measured with the pycnometer.**

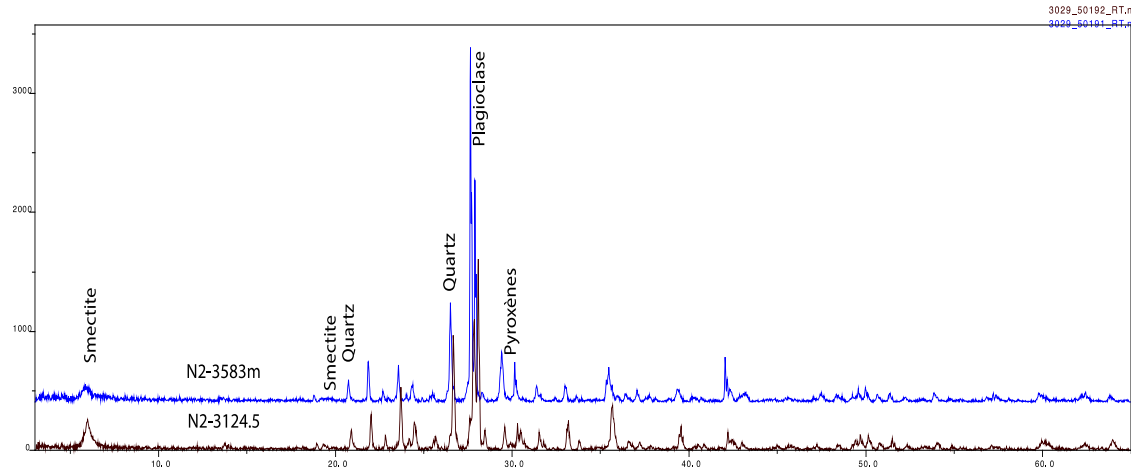


**Figure 2: Powder X-ray diffraction patterns of two basalt samples from well GEO-N2. Sample 3124 was visually fresh and 3583 was visually heavily altered. The mass fraction that could not be determined is respectively 27 and 18.5%.**

## 2.2 The Target triaxial apparatus

In order to conduct this investigation into the brittle-ductile behavior of NBB, we use the newly developed gas, Paterson-type, triaxial press TARGET installed at EPFL in Lausanne, Switzerland. The TARGET apparatus is based on the combination of a high-pressure, internally heated pressure vessel commonly used in experimental petrology (Edgar, 1973) with an axial deformation system. It allows for conditions relevant to SHR reservoirs.

In TARGET, the confining medium is applied via a gas-booster and an intensifier which can accurately generate pressures up to 400 MPa. The confining medium is argon, a gas that is chemically inert. Samples are isolated from the confining medium by a copper jacket.

The pressure vessel houses a Kanthal furnace that is divided in three coils which can be heated separately and/or concurrently with different power outputs. This design permits to heat  $40 \times 20$  mm samples up to  $800$  °C with a minimal gradient (less than  $30$  °C between the top and bottom of the sample at  $800$  °C, see Violay et al., in prep.).

Axial load is applied externally via a self-compensated ram by a 1000 kN piston. On 20 mm diameter samples, this system allows for differential stresses as high as 3 GPa. The applied load is read both externally by a load cell in the driving unit and within the pressure vessel by a semi-internal force transducer. The contribution of the copper jacket to sample strength is corrected.

Axial deformation is measured independently by two Linear Vertical Differential Transformers (LVDT): one external to the pressure vessel and one within the driving mechanism of the piston. Sample shortening is corrected from the distortion of the loading column.

A pore pressure system fed by two servo-controlled 80 mL pumps allows for fluid circulation (argon, water or brine) and can operate up to pore pressures of 300 MPa. These pumps can be controlled in harmonic mode, allowing for the application of pressure oscillations. When recording permeability, pressure oscillations of 5 MPa are applied with a period of 30 minutes on the top of the sample (upstream) while the resulting response is recorded in the downstream reservoir. The permeability is then inverted using the harmonic method (Bernabé et al., 2006; Fischer, 1992; Mitchell & Faulkner, 2008).

## 3. PRELIMINARY RESULTS AND DISCUSSION

### 3.1 Hydrostatic tests

We tested the relationship between confinement and permeability by hydrostatically loading a sample from 4014 foot depth (Figure 3). Samples were placed under confinement before pore pressure was raised to its target value of 50 MPa. The effective confining pressure steps were 30, 40 and 50 MPa. Each pressure step, a 5 MPa amplitude and 30 minutes period oscillation was applied to the upstream reservoir by the pump while the downstream response was recorded. We waited for five pore pressure cycles to be complete before proceeding with the following confining pressure step.

We observe that, in NBB, permeability remains relatively constant, marking only a slight drop from  $8.3 \times 10^{-20}$  m<sup>2</sup> at 30 MPa to  $5 \times 10^{-20}$  m<sup>2</sup> at 50 MPa.

Similarly, we conducted a study of the temperature effect on permeability by increasing temperature step-wise while keeping the effective confining pressure at 50 MPa (Figure 4). Every step, a 5 MPa oscillation with a period of 30 minutes was applied to the upstream reservoir and maintained for 5 cycles before proceeding with the following step.

Data show a marked drop from its value of  $5 \times 10^{-20} \text{ m}^2$  at 50 MPa and room temperature to  $3 \times 10^{-21} \text{ m}^2$  at 300 °C. At 400 °C, permeability is  $6.54 \times 10^{-21} \text{ m}^2$ . Further investigation into higher temperatures was halted by a jacket puncture.

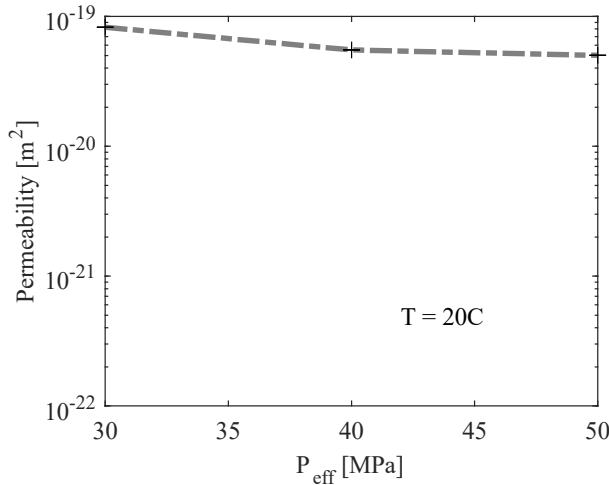


**Figure 3: Permeability as a function of effective confining pressure in a sample of NBB at 20 °C. Each permeability data point was derived using the harmonic method based on five cycles.**

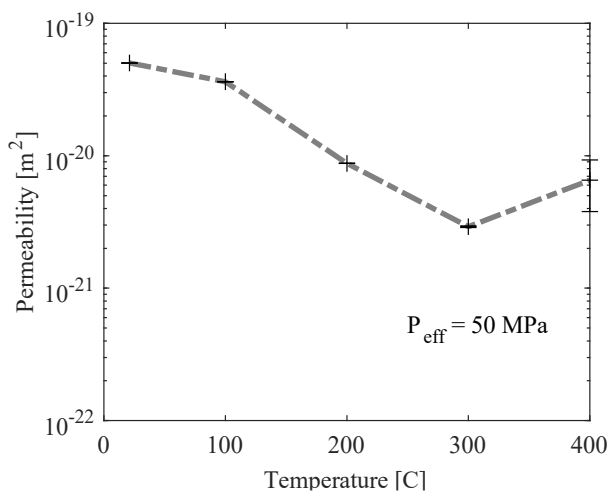


**Figure 4: Permeability as a function of temperature in a sample of NBB subjected to an effective confinement of 50 MPa. Each permeability data point was derived using the harmonic method based on five cycles.**

The somewhat pressure insensitive behavior of permeability might show that porosity in NBB is mostly comprised of rounded pores (harder to close) rather than cracks. Further microstructural analysis would be needed to confirm this hypothesis.

Conversely, permeability is sensitive to temperature. At 400 °C and only 50 MPa effective confining pressure, it has already decreased by almost an order of magnitude. We interpret this result as being the result of plastic creep processes being thermally activated which would mean that NBB could be prone to time-dependent creep. However, it is important to point here that these data are very early stage: the contribution of the jacket to the system permeability, whilst probably being negligible, is still not fully constrained and could have impacted the present results.

Overall, this porosity collapse at moderate pressure and temperature in NBB might explain the porosity collapse around 3900 feet depth observed in the well (Figure 1) were the conjoined effect of temperature and pressure at this depth could have led to porosity collapse. Further comparison with well logs will allow us to determinately conclude.

### 3.2 Deformation tests — dry

In order to constrain the rheology of NBB, we conducted dry (i.e., no pore pressure) deformation experiments at temperatures ranging from 300 to 500 °C, at a constant confining pressure of 100 MPa and constant strain rate of  $10^{-5} \text{ s}^{-1}$ .

For this series of tests, we chose samples from 4343 feet deep. This choice was motivated by the number of samples that could be extracted from this section of core (5), by the low porosity and apparent homogeneous nature of the samples below 4000 feet, and by the lack of visible alteration, preexisting cracks or veins (Figure 5 A.).

The samples showed brittle failure at all tested temperatures characterized by a visible fracture (Figure 5 B.), a shear drop in stress at the moment of rupture (Figure 6) and an audible sound. The generated macroscopic fracture spans almost the height of the sample and is ideally oriented at an angle of about 30° with respect to the direction of loading (Figure 5 B.).

At 300 °C, stress increases with strain first linearly up to 1.3 % (elastic) strain before yield occurs (Figure 6). Stress then continues increasing until it reaches 387 MPa at 2.35 % strain. At this point, stress drops brutally as the sample failed in a brittle manner.

At 400 °C, the sample is elastic up to roughly 1.5 % strain, and fails at 237 MPa and 2% strain (Figure 6). It is important to note here that the saw tooth-like spikes in stress have an experimental origin rather than being rooted in the sample deformation itself. In fact, these were caused by the refills of the intensifier, compensating for a leak that occurred during the warming up process. Given the importance of each sample, it was decided to continue the experiment, we believe these slight stress perturbations did not impact the overall mechanical behavior of the sample.

At 500 °C, yielding of the sample occurs around 1% strain (Figure 6). From this point, stress keeps on increasing up to 2.8% strain where it proceeds to plateau around 410 MPa. After a further 0.45% strain, the sample fails catastrophically.

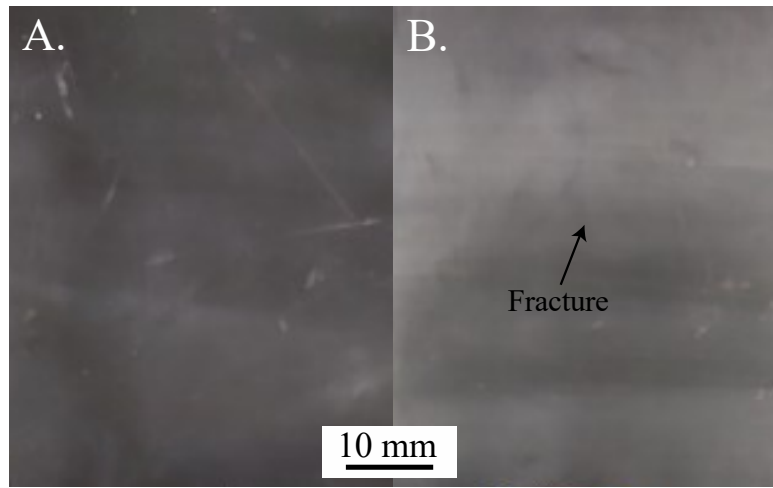


**Figure 5:** A. An intact sample of NBB originating from 4343 feet deep. B. A sample of NBB from 4343 feet deep in its copper jacket after being deformed at 300°C, 100 MPa confining pressure and constant strain rate of  $10^{-5} \text{ s}^{-1}$ .

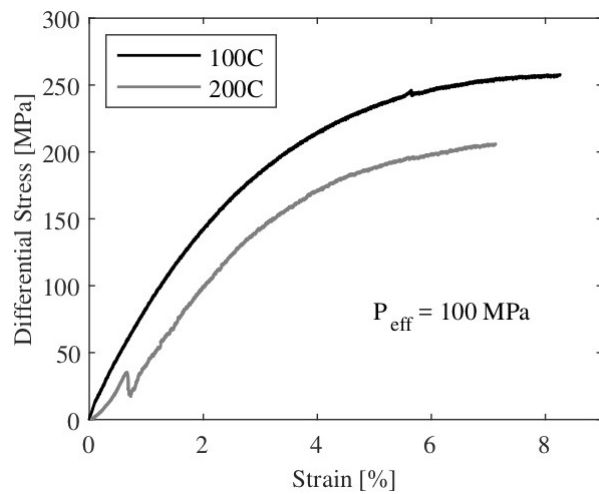


**Figure 6:** Stress evolution as a function of strain for samples of NBB originating from 4343 feet deep and deformed at different temperatures. All experiments were carried out dry (no pore pressure) and at a confining pressure of 100 MPa and constant strain rate of  $10^{-5} \text{ s}^{-1}$ .

These results are somewhat puzzling in that they do not follow the general trend of brittle-ductile transitioning rocks. Generally, higher pressure and temperature in transition rock translate to lower strength and higher strain to failure (ductility). Here the sample deformed at 500 °C is the strongest. We interpret these data as being the result of sample variability. While upon visual inspection, the sample looked similar, some sparse alteration vesicles could still be spotted. The role of such imperfections is poorly known and could result in drastically different strength and/or brittle-ductile behavior.

### 3.3 Deformation tests — with pore fluid

Additionally, we deformed two cores of NBB from the section at 4014 feet. The experiments were carried out at 100 and 200 °C, at a confining pressure of 150 MPa and a pore pressure of 50 MPa. During the entire duration of the experiments, a pore pressure oscillation of 5 MPa in amplitude and 30 minutes in period was applied to the samples. In order to have enough pore pressure cycles, the experiments were carried out at a strain rate of  $10^{-6} \text{ s}^{-1}$ , i.e., one order of magnitude lower than that applied during the dry tests.

We chose this section for the large number of samples available (5) but also for its close visual resemblance with the section from 4343 feet (Figure 7 A.).

All samples were ductile: they did not display any form of localized strain (i.e., fracture, Figure 7 B) and no stress drops were recorded during deformation (Figure 8). The perturbation in the data at 200 °C was caused by the refill of the intensifier.

After the initial elastic domain, stress increased rapidly up to about 3% strain where it rolled over and reached final values of 250 and 200 MPa at 100 and 200 °C respectively (Figure 8).

In the sample deformed at 100 °C, permeability rapidly decreased with strain from its initial value of  $6.20 \times 10^{-20} \text{ m}^2$  down to  $2.4 \times 10^{-22} \text{ m}^2$  around 5% strain (Figure 9). It decreased further beyond measurable levels and remained so up to 8% strain. Below  $10^{-21} \text{ m}^2$ , the values of permeability are unreliable given they are of the same order of magnitude as the measurement errors.

In the sample deformed at 200 °C, permeability vanished during the warming up process and remained below measurable levels over the entire deformation process. For this reason, it does not appear in Figure 9.

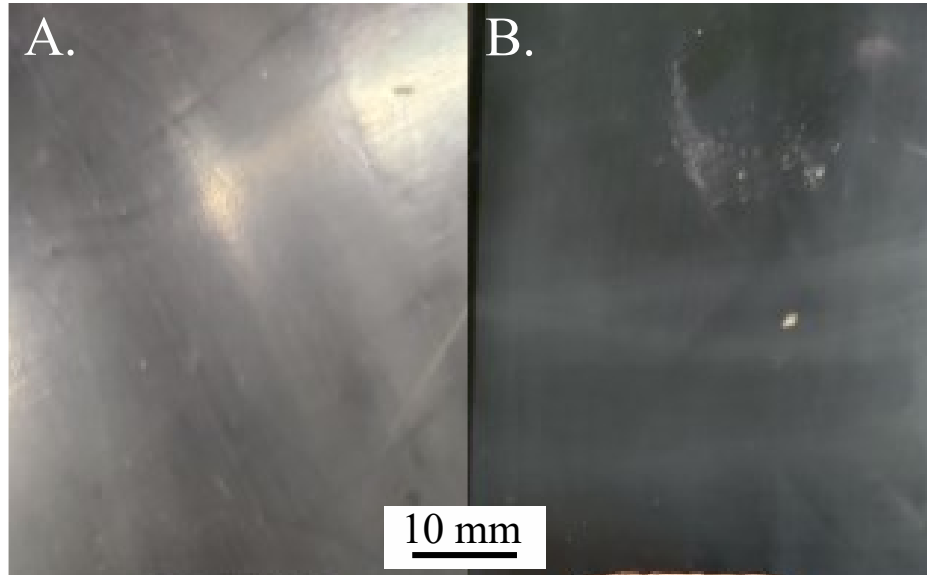


**Figure 7: A.** An intact sample of NBB originating from 4014 feet deep. **B.** A sample of NBB from 4014 feet deep in its copper jacket after being deformed at 100 °C, 100 MPa effective confining pressure and constant strain rate of  $10^{-6} \text{ s}^{-1}$ .

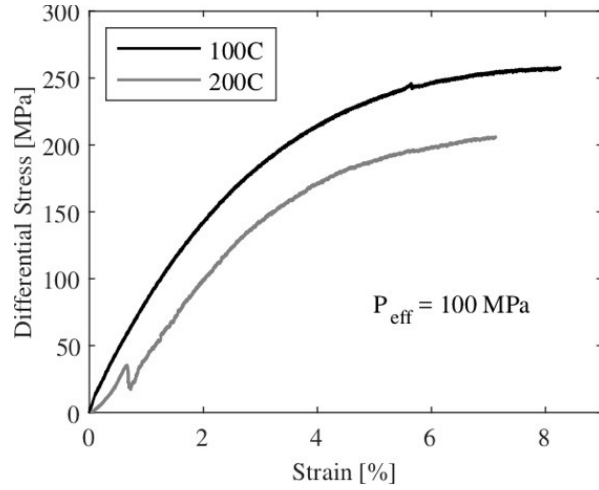


**Figure 8:** Stress evolution as a function of strain for samples of NBB originating from 4014 feet deep and deformed at different temperatures. All experiments were carried out at a confining pressure of 150 MPa, a pore pressure of 50 MPa and constant strain rate of  $10^{-6} \text{ s}^{-1}$ .

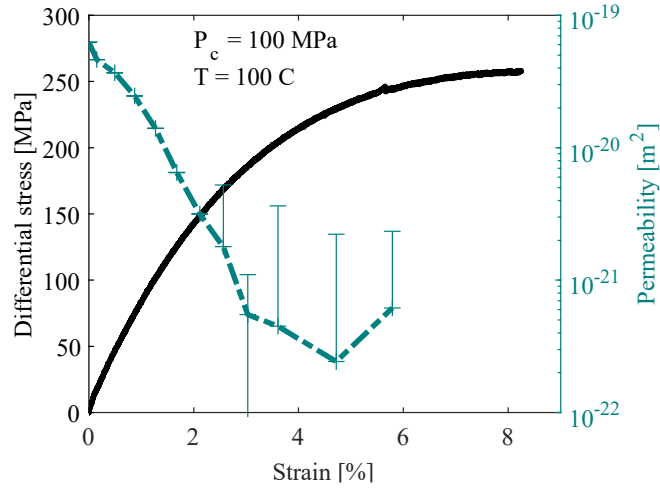


**Figure 9:** Black: stress evolution as a function of strain for a sample of NBB originating from 4014 feet deep and deformed at a confining pressure of 150 MPa, a pore pressure of 50 MPa, a temperature of 100 °C and constant strain rate of  $10^{-6} \text{ s}^{-1}$ . Turquoise: Permeability evolution as a function of strain during the same experiment. Permeability was too small to be recorded beyond 6% strain. All permeability data have been obtained with the harmonic method on five cycles (oscillations of 5 MPa amplitude and 30 minutes period).

It appears that, in ductile NBB, permeability rapidly collapses with strain. Porous volcanic rocks in the ductile regime have been shown to undergo compaction, a process during which pores collapse, closing potential pathways (Heap et al., 2017). Moreover, our hydrostatic data tend to show that NBB might be prone to viscous creep. For these reasons, we interpret the decrease in permeability as a conjoined effect of ductile pore collapse and viscous creep of the vitreous matrix.

The second observation we derive from these data is that one, if not the greatest, control of NBB rheology is strain rate. Decreasing strain rate from  $10^{-5} \text{ s}^{-1}$  to  $10^{-6} \text{ s}^{-1}$  nearly halved the samples strength and changed the overall macroscopic deformation behavior. By deforming slowly, it is possible to obtain fully ductile behavior at 100°C. This result is surprising and might open a way for future high strain rate reservoir stimulation, but further work is required to confirm this conclusion as the data presented here are very immature.

#### 4. CONCLUSION

We conducted deformation experiments on basalts from corehole GEO-N2 from the west flank of Newberry Volcano, Oregon adjacent to the Newberry SHR geothermal project. We showed that, in this basalt, porosity is nonexistent below 3900 ft.

By conducting hydrostatic experiments, we showed that permeability in NBB is rather pressure independent, a fact we interpret as being rooted in the shape of the pores: round rather than elongated cracks. On the other hand, we showed that permeability is very sensitive to temperature. We believe temperature activates ductile processes leading eventually to pore collapse.

Additionally, at a strain of  $10^{-5} \text{ s}^{-1}$  and  $P_c$  of 100 MPa, NBB is brittle at least up to 500 °C but the overall strength of the samples appears random. We tentatively concluded that sample variability might be involved, a fact that could reveal itself as a hindrance to a thorough mechanical investigation of the BDT of NBB.

Our experiments with pore pressure showed that permeability rapidly decreases during ductile deformation of NBB and remains below  $10^{-22} \text{ m}^2$  for strain as high as 8%. We interpret this as an effect of pore collapse and matrix deformation during ductile flow. If cracks do form, the ductile nature of deformation prevents them from coalescing and hence from forming flow paths.

Finally, we showed that the BDT of NBB is highly strain rate dependent. A decrease of strain rate by an order of magnitude was sufficient to induce ductile deformation at 100 °C and  $P_c$  of 100 MPa. This extremely early result could indicate that rapid reservoir stimulation might be able to embrittle the ductile carapace of magma bodies and hence transition SHR reservoirs from impermeable ductile deformation to potentially brittle, flow path forming, deformation. However, at this stage of our investigation, this conclusion is purely speculative and should not be considered a grounded fact.

In the future, we plan on conducting a thorough microstructural study of deformed and intact samples with the aim of confirming the vitreous nature of NBB and the extent of alteration in the samples as well as identifying the ductile processes involved in the permeability reduction. Concurrently, we will continue to populate the permeability data and the mechanical data to establish an entire rheological envelope for NBB. Once the behavior of argon permeability through the brittle ductile transition will be fully constrained, we plan on moving to water permeability and assess the hydraulic properties of NBB.

## REFERENCES

- Bernabé, Y., Mok, U., & Evans, B. (2006). A note on the oscillating flow method for measuring rock permeability. *International Journal of Rock Mechanics and Mining Sciences*, 43(2), 311–316.
- Bignall, G., & Carey, B. (2011). A deep (5km?) geothermal science drilling project for the Taupo Volcanic Zone—Who wants in. *Proceedings 33rd New Zealand Geothermal Workshop*.
- Cladouhos, T. T., Petty, S., Bonneville, A., Schultz, A., & Sorlie, C. F. (2018). Super hot EGS and the Newberry deep drilling project. *43rd Workshop on Geothermal Reservoir Engineering, Stanford University, Stanford, California*.
- Driesner, T., & Geiger, S. (2007). Numerical simulation of multiphase fluid flow in hydrothermal systems. *Reviews in Mineralogy and Geochemistry*, 65(1), 187–212.
- Edgar, A. D., & Edgar, A. D. (1973). *Experimental petrology: Basic principles and techniques*. Oxford: Clarendon Press.
- Elders, W. A., Friðleifsson, G., & Albertsson, A. (2014). Drilling into magma and the implications of the Iceland Deep Drilling Project (IDDP) for high-temperature geothermal systems worldwide. *Geothermics*, 49, 111–118.
- Fischer, G. J. (1992). The determination of permeability and storage capacity: Pore pressure oscillation method. In *International Geophysics* (Vol. 51, pp. 187–211). Elsevier.
- Fournier, R. O. (1999). Hydrothermal processes related to movement of fluid from plastic into brittle rock in the magmatic-epithermal environment. *Economic Geology*, 94(8), 1193–1211.
- Friðleifsson, G., Elders, W. A., & Albertsson, A. (2014). The concept of the Iceland deep drilling project. *Geothermics*, 49, 2–8.
- Hayba, D. O., & Ingebritsen, S. E. (1997). Multiphase groundwater flow near cooling plutons. *Journal of Geophysical Research: Solid Earth*, 102(B6), 12235–12252.
- Heap, M. J., Violay, M., Wadsworth, F. B., & Vasseur, J. (2017). From rock to magma and back again: The evolution of temperature and deformation mechanism in conduit margin zones. *Earth and Planetary Science Letters*, 463, 92–100.
- Jolie, E., Scott, S., Faulds, J., Chambefort, I., Axelsson, G., Gutiérrez-Negrín, L. C., Regenspurg, S., Ziegler, M., Ayling, B., & Richter, A. (2021). Geological controls on geothermal resources for power generation. *Nature Reviews Earth & Environment*, 2(5), 324–339.
- Mitchell, T. M., & Faulkner, D. R. (2008). Experimental measurements of permeability evolution during triaxial compression of initially intact crystalline rocks and implications for fluid flow in fault zones. *Journal of Geophysical Research: Solid Earth*, 113(B11).
- Prejean, S. G., & Haney, M. M. (2014). Shaking up volcanoes. *Science*, 345(6192), 39–39.
- Scott, S., Driesner, T., & Weis, P. (2015). Geologic controls on supercritical geothermal resources above magmatic intrusions. *Nature Communications*, 6(1), 1–6.
- Weis, P. (2015). The dynamic interplay between saline fluid flow and rock permeability in magmatic-hydrothermal systems. *Geofluids*, 15(1–2), 350–371.